Research Article | Vol. 24, No. 21 | 17 Oct 2016 | OPTICS EXPRESS 24232

Optics EXPRESS

Design, fabrication and characterization of transparent retro-reflective screen

SHOAIB R SOOMRO* AND HAKAN UREY

Optical Microsystems Laboratory, Electrical Engineering Department, Koç University Rumelifeneri Yolu, 34450 Sariyer, Istanbul, Turkey

ssoomro13@ku.edu.tr

Abstract: A transparent retro-reflective screen, which can be used as head-up-display (HUD) or a see-through screen for head mounted projection displays (HMPD) is proposed. The high optical gain of screen enables the use of low power projectors to produce very bright content. The screen assembly is based on retro-reflective microspheres, patterned on an optically clear substrate using steel stencil as a shadow mask. The incident light is retro-reflected as a narrow angular cone to create an eyebox for the viewer. The optical gain and transparency of screen is varied by changing the fill factor of the mask. The optical design and fabrication of the screen is presented. The retro-reflective and transmission characteristics of screen are evaluated. The impact of fill factor on screen luminance and transparency is studied. The screen provides high luminance (up to 280cd/m^2 with 50% transparency) from about 40cm to >3m when used with a low power (15 lumen) mobile projector. Unlike regular diffusers, luminance remains nearly constant with projection distance. Furthermore, the screen offers prominent see-through capability with small degradation in modulation transfer function for transmitted light. For a particular camera and imaging configuration, MTF10 (10% cutoff) for 50% transparent screen is reduced from 37 cyc/deg to 30 cyc/deg when screen is inserted at an intermediate distance.

OCIS codes: (220.0220) Optical design and fabrication; (130.3990) Micro-optical devices; (120.2040) Displays.

References and links

1. G. Patrick, M. Sander, J. Meyer, M. Kröger, E. Becker, H. H. Johannes, W. Kowalsky, and T. Riedl, "Towards see-through displays: fully transparent thin-film transistors driving transparent organic light-emitting diodes," Adv. Mater. **18**(6), 738–741 (2006).
2. C. W. Hsu, B. Zhen, W. Qiu, O. Shapira, B. G. DeLacy, J. D. Joannopoulos, and M. Soljačić, "Transparent displays enabled by resonant nanoparticle scattering," Nat. Commun. **5**, 3152 (2014).
3. M. K. Hedili, M. O. Freeman, and H. Urey, "Transmission characteristics of a bidirectional transparent screen based on reflective microlenses," Opt. Express **21**(21), 24636–24646 (2013).
4. K. Hong, J. Yeom, C. Jang, G. Li, J. Hong, and B. Lee, "Two-dimensional and three-dimensional transparent screens based on lens-array holographic optical elements," Opt. Express **22**(12), 14363–14374 (2014).
5. K. Hong, J. Yeom, C. Jang, J. Hong, and B. Lee, "Full-color lens-array holographic optical element for three-dimensional optical see-through augmented reality," Opt. Lett. **39**(1), 127–130 (2014).
6. D. Héricz, T. Sarkadi, V. Lucza, V. Kovács, and P. Koppa, "Investigation of a 3D head-mounted projection display using retro-reflective screen," Opt. Express **22**(15), 17823–17829 (2014).
7. P. Harman, "Retroreflective screens and their application to Autostereoscopic displays," Proc. SPIE **3012**, 145–153 (1997).
8. H. Hua, C. Gao, and J. P. Rolland, "Imaging properties of retroreflective materials used in head-mounted projective displays (HMPDs)," Proc. SPIE **4711**, 194–201 (2002).
9. J. Lloyd, "A brief history of retroreflective sign face sheet materials," The Retroreflective Equipment Manufacturers Association: Lancashire, UK http://www.rema.org.uk/. Accessed on 11th January 2016.
10. J. J. Snyder, "Paraxial ray analysis of a cat's-eye retroreflector," Appl. Opt. **14**(8), 1825–1828 (1975).
11. Colesafety International, "Reflective glass microbeads," http://www.colesafety.com/Reflective-Glass-Beads-Type-I_c17.htm.
12. W. J. Smith, *Modern Optical Engineering* (McGraw-Hill, 2000), Chap. 8.
13. P. M. Estribeau, "Fast MTF measurement of CMOS imagers using ISO 12233 slanted edge methodology," Proc. SPIE **5251**, 243–252 (2004).
14. J. Canny, "A computational approach to edge detection," IEEE Trans. Pattern Anal. Mach. Intell. **6**, 679–698 (1986).

#273310 http://dx.doi.org/10.1364/OE.24.024232
Journal © 2016 Received 11 Aug 2016; revised 6 Oct 2016; accepted 6 Oct 2016; published 11 Oct 2016

Optics EXPRESS

1. Introduction

Transparent displays are widely investigated for many useful applications. Their ability to overlay virtual objects on the top of real-world scene make them an ideal choice for augmented reality applications. Transparent screens can be used as head-up-display (HUD) to display navigational information on vehicle windshields, a see-through screen for head mounted projection displays (HMPD) and floating display for smart windows and advertisements.

The concept of transparent displays has been explored in several ways. Active transparent displays have been investigated using light emitting diodes [1], however such displays offer limited transparency and are hard to fabricate in large format. Projection based transparent displays have also been demonstrated. A non-transparent diffused screen (i.e. Lambertian scatterer) provides isotropic luminance in full hemisphere and is considered to have an optical gain of 1. High optical gain is important for transparent screens specially when used for mobile applications and high ambient environments due to their inherent transmission loss. Transparent projection screens are constructed using several different techniques. Wavelength selective scattering screen is developed by embedding resonant nano-particles into the clear glass [2], the nano-particles scatter only selected color wavelength and transmit other colors. Such screens can provide enhanced transparency but are limited to single color operation. Index matched partially reflective microlens arrays [3] have been used to build transparent screens where micro-lenses scatter the part of incident light and create the eyebox for the viewer, while the remaining light is transmitted through partial coating. Such screens usually suffer from lower gain and cannot provide significant transparency. Transparent screens using lens arrays recorded on holographic material films have also been demonstrated [4,5], however holographic film have poor transparency and are hard to fabricate and operate in large format. A retro-reflective surface reflects incident light back towards source with narrow scattering. The retro-reflective surfaces have been demonstrated as light efficient screens for HMPDs and HUDs and autostereoscopic displays due to their narrow angle scattering capabilities [6–8].

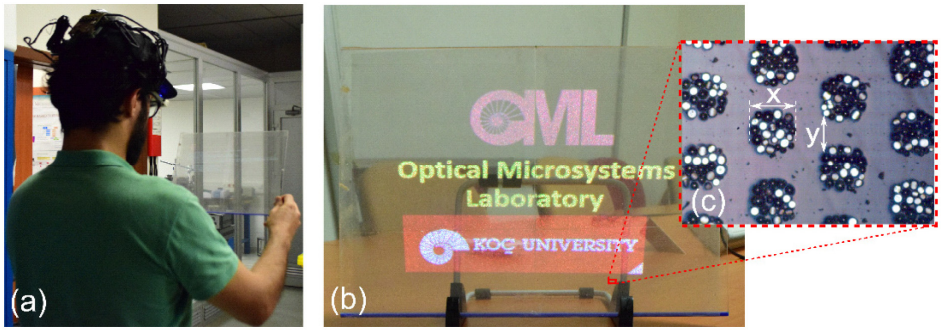

Fig. 1. (a) A viewer using transparent retro-reflective screen with a laser pico projector based HMPD, (b) shows the perceived content when viewer's eye is close to projector, and (c) microscopic view of screen (75% transparent) showing retro-reflective microspheres.

In this paper, we present a transparent retro-reflective screen, which can be used to display bright content while maintaining the high transparency as shown in Fig. 1. The proposed screen uses retro-reflective microspheres micro-patterned on an optically clear substrate. The retro-reflective material directs significant amount of incident light towards source and enables the user to perceive high luminance, when viewer's eyes are located in closed proximity of projector [Fig. 1(a)]. This makes the proposed screen an ideal choice for the applications where viewer has limited movement with respect to projector (i.e. HUDs and HMPDs). To the best of our knowledge, the proposed screen is first transparent retro-reflective screen in the literature. We developed different versions of transparent retro-

Optics EXPRESS

reflective screen providing different levels of optical gain and transparency. This paper presents the design and fabrication process of screen and evaluates the display and transmission performance of developed screen, Section-2 explains the design of screen, Section-3 presents the fabrication process, while Section-4 and Section-5 examine the various display and transmission characteristics of screen respectively.

2. Transparent screen design

The proposed screen makes use of retro-reflective microspheres in the form of perforated micro-patterns to direct the light towards its source. A 100% fill-factor retro-reflective surface can provide optical gain of 10-1000 within the particular viewing range [6]. The amount of retro-reflective material on an optically clear surface can be controlled to create see-through and retro-reflective regions. Significant display gain and enhanced transparency can be achieved by optimizing the surface filling. To minimize the visibility of structural artifacts on the screen surface, the feature size of micro-pattern can be made small enough to be irresolvable by naked eye at a typical working distance from the screen.

Assuming 1 arc minute angular resolution for the human eye and a working distance of > 40 cm, a pattern size below 100-150 μm is not visible to the eye. Since the pattern features are small enough to be resolved by human eye, different geometric shapes including circular, triangular and hexagonal can be used to make the retro-reflective micro-pattern. In the presented implementation, we used square shaped patches of size (x) 100μm to create micro-patterns as shown in Fig. 1(c).

To investigate the impact of surface filling on optical gain and transparency, we developed three different versions of screen having fill factor of 50%, 25% and 10% providing the screen transparencies of 50%, 75% and 90% respectively. Since the 100μm feature size was the minimum achieved with the laser micromachining tool used for mask production, the feature size (x) was kept same in all designs, while the gap (y) between retro-reflective islands was varied to change the transparency (T) as follows:

$$T = 1 - \frac{x^2}{(x+y)^2} \tag{1}$$

There are various types of retro-reflective materials used for projection screens and road safety applications [8,9]. Our design utilizes cat's eye retro-reflectors [10]. We used high refractive index microspheres having half-shell coated with aluminum to create retro-reflective patterns. Compared to an ideal retro-reflector, which retro-reflects incident light without diverging, a microspheres based retro-reflector spreads incident light towards source creating a narrow angular cone, which defines the eyebox of the display. The width of the cone depends on refractive index and size of the microspheres, lower refractive index and smaller size of microspheres leads to an expanded cone (due to geometric optics and diffraction effects). We use titanium dioxide glass microspheres having the refractive index of ≈1.93 and half-shell aluminum coating. The size distribution of microspheres is 35-45μm with mean a diameter of 40μm [11]. The perceived luminance of display increases significantly when viewer moves close to the projector. The detailed retro-reflective properties of screen are discussed later.

3. Screen fabrication

Figure 2 illustrates the fabrication process of the transparent retro-reflective screen. First, an optically clear thin (200μm) flexible acrylic substrate (Poly methyl methacrylate used as LCD protection film) was cleaned and prepared. In the second step, a 10-20μm thick uniform coating of optical adhesive was applied on the substrate. Both pressure sensitive optically clear adhesive film (used for smartphone LCD glass repair) and UV curable liquid adhesive (Norland adhesives) were tested. The pressure sensitive adhesive was applied to substrate in

Optics EXPRESS

the form of thin film, while UV curable epoxy was deposited using spin coating. Both types of adhesive performed up to mark, while pressure sensitive adhesive was preferred due to its better mask alignment and release. In the third step, a thin mask (steel stencil) with perforated square holes was bonded to the substrate as shadow mask. The stencil was designed in-house and was produced using the laser micromachining tools by availing the services from standard PCB stencil manufacturing companies. In the next step, the retro-reflective microspheres having hemispherical (half-shell) aluminum coating were randomly sprinkled on to the mask using a powder shaker container to fill perforations and microspheres were bonded to substrate by applying external pressure using a hand roller (typically used for LCD polarizer lamination). In the last step, the mask was peeled-off from substrate by separating the substrate and steel stencil and retro-reflective microspheres remained on the surface providing transparent retro-reflective screen. For pressure sensitive adhesive, we did not notice any visible traces of adhesive transferred to stencil and the retro-reflective pattern was neatly transferred to the substrate as seen in microscopic image [Fig. 1(c)]. For the UV curable liquid adhesive, a small gap between stencil and substrate was maintained by attaching scotch tape on stencil boundaries to separate the mask and adhesive.

The mask (stencil) of size 8x8 cm^2 was used for fabrication and the large sized screen (up to 30x20 cm^2) was constructed by fabricating the 8x8 cm^2 screen segments individually and then tiling them together. To increase the transparency of screen, a different stencil mask with reduced fill factor was used, while the fabrication process was kept same. The screens of larger size and variable aspect-ratio can be constructed by tiling together the increased number of segments.

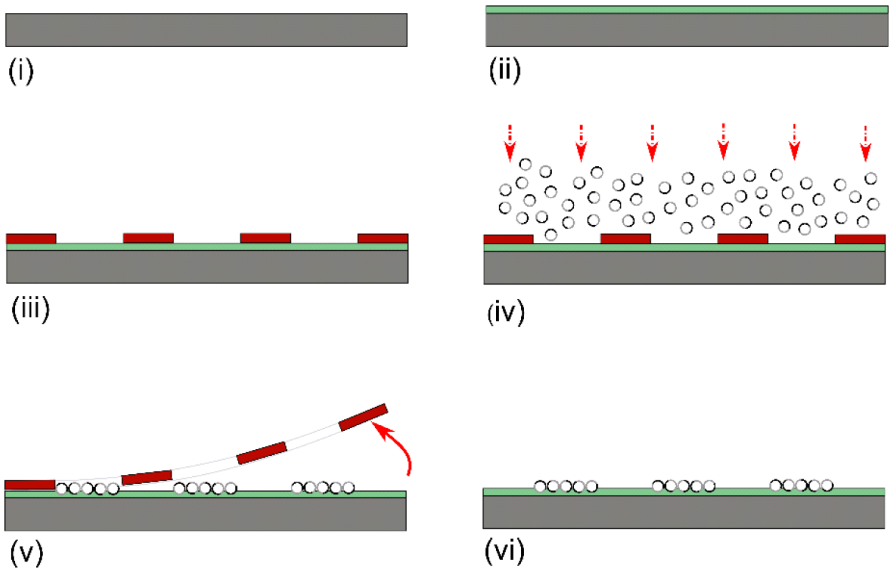

Fig. 2. Illustrates the fabrication process of transparent retro-reflective screen, (i) optically clear substrate (200 µm) preparation, (ii) thin (20 µm) adhesive coating, (iii) flexible mask (steel stencil) bonding and alignment, (iv) retro-reflective microspheres raining, (v) mask removal, and (vi) transferred periodic pattern with retro-reflective microspheres.

4. Retro-reflective characteristics

4.1 Coefficient of retro-reflectivity

Retro-reflective coefficient can be defined as the amount of retro-reflected light as function of viewing angle. The transparent retro-reflective screen reflects incident light towards source in the form of angular cone. The distance between eye and projector s, and distance between viewer and screen d defines the viewing angle α, which can be expressed as:

Optics EXPRESS

$$\alpha = \tan^{-1}\left(\frac{s}{d}\right) \tag{2}$$

Equation (2) indicates that viewing angle decreases with increasing viewer-to-screen distance and decreasing eye-to-projector distance. When the viewing angle is minimized the viewer's eye moves towards the peak of retro-reflective cone and perceived brightness is significantly increased.

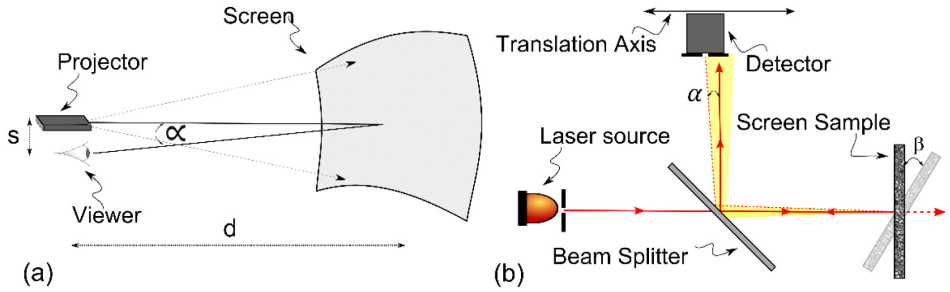

Fig. 3. (a) Illustrates the viewing angle formed by viewer's eye with respect to screen and projector, and (b) shows the illustration of photometric setup used to measure the retro-reflective coefficient of transparent screen.

In order to determine the coefficient of reflectivity of developed screen, the intensity of reflected light as function of viewing angle is measured. A photometric setup was constructed as illustrated in Fig. 3(b). The sample of transparent retro-reflective screen was illuminated with a collimated 632.8 nm HeNe laser at 0° incident (β = 0). The occlusion due to detector was prevented by using a 50/50 beam splitter between screen and detector. To limit the size of collimated laser beam, a 1 mm diameter aperture was placed in front of laser source. The retro-reflected intensity at different angular positions is measured using a power meter (PM100A Thorlabs). The distance between sample screen and detector was kept as 21 cm to record the detected power within ± 3° viewing angle. The detector having a diameter of 1.5 mm is placed on a translation stage to allow precise movement across retro-reflective cone. An angular step size of 0.14° was achieved by moving detector with 500 μm steps. The retro-reflective coefficient of transparent screen is calculated as follow:

$$R_c(\alpha) = \frac{P_d(\alpha)}{0.5 \times P_s} \tag{3}$$

Where is the detected power at viewing angle (α), is the input beam power measured at sample position and is the resultant retro-reflective coefficient. Figure 4 shows the measured retro-reflective coefficient for three different versions of transparent screens providing 50%, 75% and 90% transparency. It can be seen that amount of retro-reflection is decreased as the transparency of screen is increased. Due to the use of same microspheres, all screen samples provide identical cone shape having approximately 2° angular width. All three curves show slight side lobes, which is the result of diffraction due to the small size of microspheres.

Optics EXPRESS

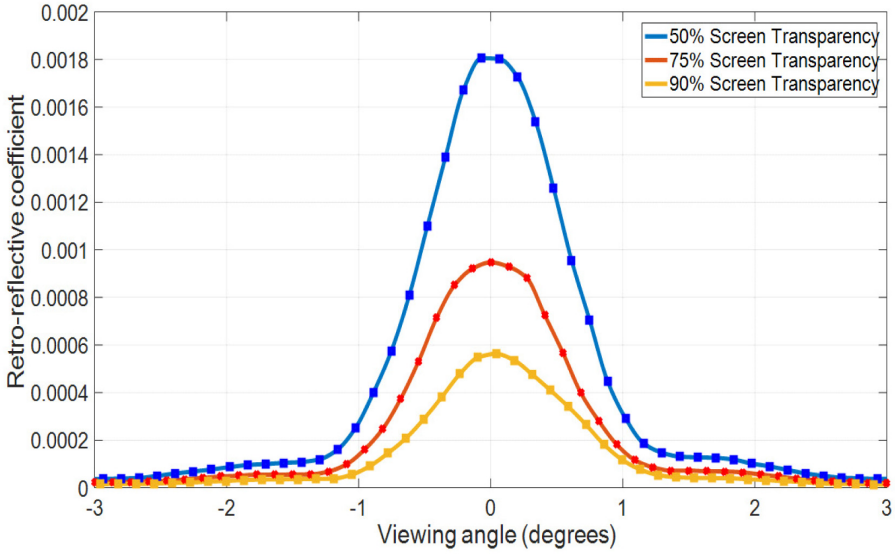

Fig. 4. Experimentally recorded retro-reflective coefficient for three different screen samples, the coefficient value is decreased with increasing screen transparency, while the shape of retro-reflective cone is unaffected.

4.2 Screen luminance

The luminance of a non-transparent diffusing screen providing equal light in all directions can be calculated as follows [12]:

$$L_d = \frac{P_l}{\pi(k \times d^2)} \tag{4}$$

Where L_d is the luminance of diffusing screen illuminated by projector having power lumens across screen area $A = k \times d^2$. For the retro-reflective screen, Eq. (4) can be modified by considering the retro-reflective coefficient information $R_c(\alpha)$ and detector solid angle (ψ) with respect to screen [6]. The modified relation can be expressed as:

$$L_r = R_c(\alpha)\frac{P_l}{\psi(k \times d^2)} \tag{5}$$

The luminance profile of transparent retro-reflective screen was obtained by putting the experimental measurement of $R_c(\alpha)$ [Fig. 4] in Eq. (5) and assuming a 15 lumen projector having 49° field of view (k = 0.538). Figure 5(a) shows the luminance curves as a function of viewer-to-screen distance for three versions of screen (50%, 75% and 90% transparency) and two different eye-to-projector distance (s) values (2 cm and 5 cm).

Optics EXPRESS

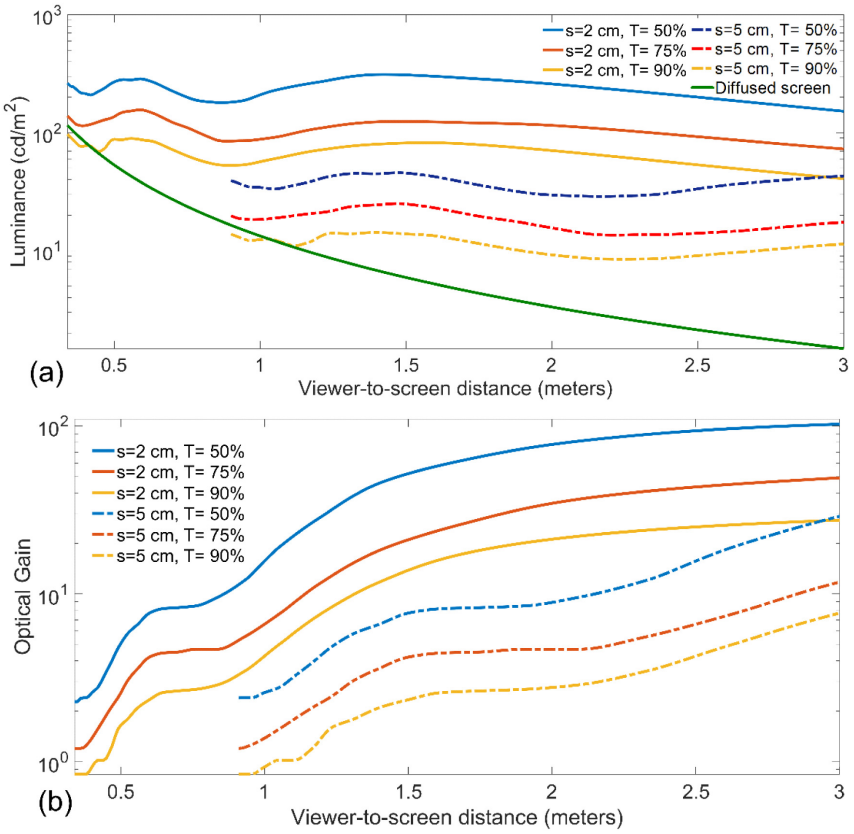

Fig. 5. Shows luminance performance (a) and optical gain (b) of three different version of screens (50%, 75% and 90% transparency) when eye-projector distance (s) is 2cm and 5cm.

Figure 5(a) shows the increased luminance at the cost of lower transparency. The screen luminance of 280 cd/m^2 is achieved with a 50% transparent screen and 2 cm eye-to-projector distance. The luminance is significantly reduced as viewer's eye moves away from the projector (compare s = 2, and s = 5). Each curve shows a luminance valley, which is the result of local diffraction minima in retro-reflective cone as seen in Fig. 4. Additionally, Fig. 5(a) shows that the screen luminance does not have exponential drop (as in diffusing screens) when viewer moves away from screen. This is due to the decline in viewing angle with increasing viewer-to-screen distance.

The optical gain of proposed screen is determined by calculating the luminance ratio between the proposed screen (L_r) and a regular non-transparent diffused screen (L_d), which can be expressed as:

$$G = \frac{L_r}{L_d} \tag{6}$$

Figure 5(b) shows the optical gain of the proposed screen for increasing screen-to-viewer distance. In contrast to diffusing screen, the luminance of proposed screen remains constant as viewer moves away from screen which results higher optical gain for larger viewer-to-screen distance. The screen shows optical gain of up to 100 at a working distance of 3 meters with 50% transparency and 2 cm eye-to-projector distance. Figure 5(b) also shows that 75% transparent version of proposed screen is more than ten times brighter than a non-transparent diffusing screen when viewed/projected from a distance of 1.5 meters.

Optics EXPRESS

Due to the retro-reflective nature of screen, no power is detected beyond ± 3° viewing angles and the luminance for larger eye-to-projector distance and closer viewer-to-screen distance cannot be measured. Since we use the microspheres having half-shell aluminum coating already, the coated side of microspheres is randomly oriented after they are bonded to substrate and only a fraction (about 30-35%) of microspheres having aluminum coating on rear side behave as retro-reflective as seen in Fig. 1(c). The bright microspheres seen in Fig. 1(c) are correctly oriented and retro-reflect the incident light successfully, while the dark microspheres are the ones oriented other way and behave as dead spots. The retro-reflective efficiency, luminance and optical gain can be further enhanced by refining the fabrication process of screen and ensuring the precise orientation of all microspheres.

4.3 Entrance angle

Luminance uniformity across screen area is an important parameter for a display screen. For retro-reflective screens, it can be characterized by entrance angle [8]. Entrance angle is defined as range of incident angles, at which screen remains highly retro-reflective. For uniform luminance, the entrance angle of transparent retro-reflective screen should be greater than the field of view of projector.

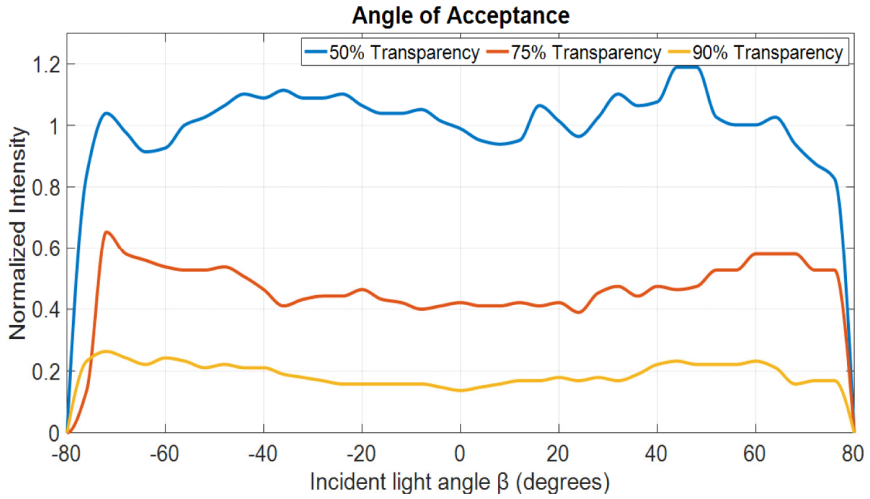

Fig. 6. Shows the entrance angle of different version of transparent retro-reflective screen. The intensity of retro-reflected light remains nearly constant within wide range of incident angles (–75 to + 75 degrees).

The entrance angle of transparent retro-reflective screen was measured by modifying the measurement setup shown in Fig. 3(b). The detector was fixed at 0° viewing angle (α = 0), while screen sample was placed on variable angular stage to vary the incident angle (β) of incoming beam. Figure 6 shows the detected power (mean normalized to 50% transparent screen) as a function of incident angle. The figure shows wider acceptance angles (–75° to + 75°) within the intensity variation of ± 10%. The effect of entrance angle plotted in Fig. 6 can also be seen in Fig. 1(b). The luminance uniformity from center to the edges of screen in Fig. 1(b) shows that the entrance angle of screen is wide enough to cover the field of view of projector. The wider acceptance angle guarantees the unprecedented luminance performance, even when the screen has sharp tilt with respect to projector.

Transmission properties

To evaluate the transparency of the developed screen, the modulation transfer function (MTF) for the light transmitted through screen was measured. Slant edge technique was used to find experimental MTF [13]. Figure 7(a) illustrates the experimental setup. A slanted edge object

Optics EXPRESS

with 3° tilt was placed at 50 cm from transparent screen. The image of edge was captured by a CCD camera located on other side at the distance of 100 cm from the screen.

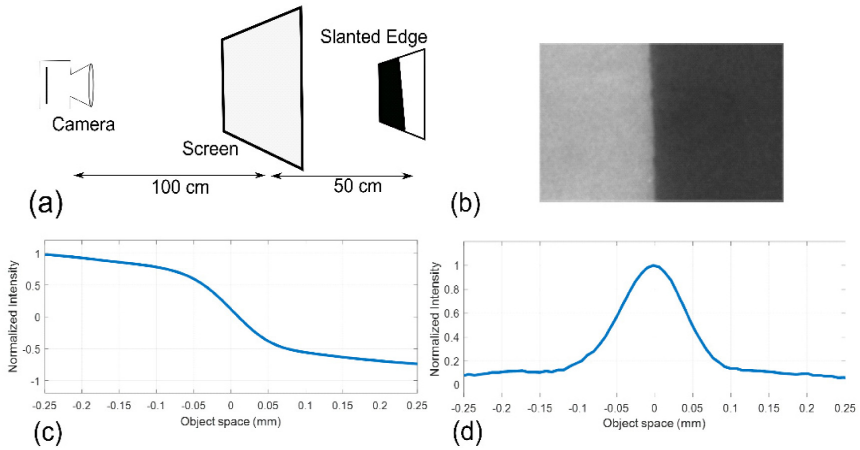

Fig. 7. (a) Shows the experimental setup used to measure transmission MTF of screen, (b) Shows the captured edge profile through 75% transparent screen, (c) shows the recovered edge spread function (ESF), and (d) shows corresponding point spread function (PSF).

Figure 7(b) shows the captured edge on camera through 75% transparent screen. First Canny edge detection technique was applied to detect the edge [14]. The angle of the slanted edge was estimated by performing line fitting of the detected edge; the image was then up-sampled by factor of four and edge was straightened by applying an affine transformation using computed edge angle. From the column average of subsequent image, an over-sampled edge profile was calculated, which is one dimensional edge spread function (ESF) shown in Fig. 7(c). The point spread function (PSF) shown in Fig. 7(d) was further calculated by computing the derivative of ESF. Finally, the transmission MTF of screen was measured by calculating the absolute value of the Fourier transform of PSF.

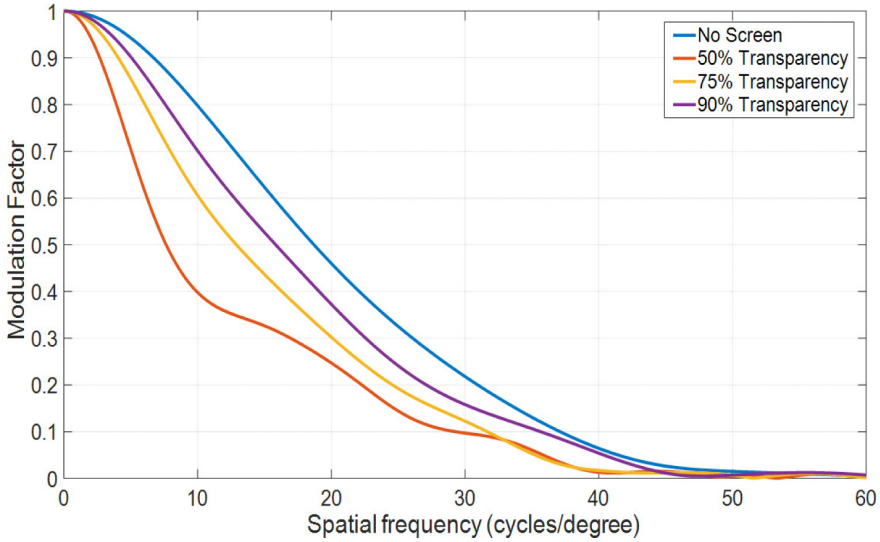

Fig. 8. Shows measured transmission MTF for changing screen transparency. MTF50 (50% cutoff) is reduced from 18 cyc/degree to 8 cyc/deg and MTF10 (10% cutoff) is reduced from 37cyc/deg to 30cyc/deg when screen transparency is decreased to 50%.

Optics EXPRESS

With this method, the MTF curves for three retro-reflective screens with different transparency levels were obtained as shown in Fig. 8. The 'no screen' MTF curve shows the MTF of the camera without having screen in between for reference. The camera f-number was configured to provide 20% cut-off at 30 cycles/degree to make it consistent with normal human vision. Figure shows reduced see-through resolution with increased fill factor. Increasing retro-reflective fill factor reduces the amount of transmitted light, which results contrast loss when looking through screen. The 90% transparent screen perform closer to reference MTF. The MTF50 (50% cutoff) is reduced to 16 cycles/degree for 90% transparent screen, 13 cycles/degree for 75% transparent screen and 8 cycles/degree for 50% transparent screen, when compared to the reference MTF (18 cycles/degree).

Conclusion

In this paper the design methodology, fabrication process, display and transmission characteristics of transparent retro-reflective screen are discussed. The use of micro-patterned retro-reflective microspheres was demonstrated as highly transparent retro-reflective screen that can project very bright content. The retro-reflective properties of screen were measured by constructing a photometric setup that was later used to calculate the screen luminance and uniformity. The optical transmission of screen was evaluated by measuring the transmission MTF of screen.

Different levels of transparency and optical gain can be achieved by controlling the proportion of the retro-reflective material on a clear substrate. The proposed screen can be used for augmented reality applications in head-up-displays and head mounted projection displays where viewers have limited mobility with respect to projector. Our results showed that at the working distance of 60 cm and eye-projector distance of 2 cm the proposed screen can provide the optical gains of 8, 4 and 2 while maintaining 50%, 75% and 90% transparency respectively. The optical gain increases significantly (up to 100 with 50% transparency) when the screen is illuminated/viewed from larger distances (3 meters). We fabricated the screen on a thin flexible substrate, which enables it to be flexible and easily installable on any clear surface (i.e. car windshields, home windows). The retro-reflective cone can be widened and retro-reflective efficiency can be improved by using smaller sized microspheres and refining fabrication process.

Funding

European Research Council (ERC) under the European Union's Seventh Framework Program (FP7/2007-2013) / ERC advanced grant agreement (340200).

Acknowledgments

We thank Muhsin Eralp and Selim Olcer for process development, Erdem Ulusoy and Sven Holmstrom for helpful discussions.